

This manuscript has been authored by UT-Battelle, LLC under Contract No. DE-AC05-00OR22725 with the U.S. Department of Energy. The United States Government retains and the publisher, by accepting the article for publication, acknowledges that the United States Government retains a non-exclusive, paid-up, irrevocable, world-wide license to publish or reproduce the published form of this manuscript, or allow others to do so, for United States Government purposes. The Department of Energy will provide public access to these results of federally sponsored research in accordance with the DOE Public Access Plan(<http://energy.gov/downloads/doe-public-access-plan>).

arXiv:2011.04477v1 [cond-mat.str-el] 9 Nov 2020

# Pressure-Induced Unconventional Quantum Phase Transition with Fractionalization in the Coupled Ladder Antiferromagnet $C_9H_{18}N_2CuBr_4$

Tao Hong,<sup>1,\*</sup> Tao Ying,<sup>2</sup> Qing Huang,<sup>3</sup> Sachith E. Dissanayake,<sup>4</sup> Yiming Qiu,<sup>5</sup> Mark M. Turnbull,<sup>6</sup> Andrey A. Podlesnyak,<sup>1</sup> Yan Wu,<sup>1</sup> Huibo Cao,<sup>1</sup> Izuru Umehara,<sup>7</sup> Jun Gouchi,<sup>8</sup> Yoshiya Uwatoko,<sup>8</sup> Masaaki Matsuda,<sup>1</sup> David A. Tennant,<sup>9</sup> Kai P. Schmidt,<sup>10</sup> and Stefan Wessel<sup>11</sup>

<sup>1</sup>*Neutron Scattering Division, Oak Ridge National Laboratory, Oak Ridge, Tennessee 37831, USA*

<sup>2</sup>*Department of Physics, Harbin Institute of Technology, 150001 Harbin, China*

<sup>3</sup>*Department of Physics and Astronomy, University of Tennessee, Knoxville, Tennessee 37996, USA*

<sup>4</sup>*Department of Physics, Duke University, Durham, North Carolina 27708, USA*

<sup>5</sup>*National Institute of Standards and Technology, Gaithersburg, Maryland 20899, USA*

<sup>6</sup>*Carlson School of Chemistry and Department of Physics,*

*Clark University, Worcester, Massachusetts 01610, USA*

<sup>7</sup>*Department of Physics, Yokohama National University, Yokohama 240-8501, Japan*

<sup>8</sup>*Institute for Solid State Physics, University of Tokyo,*

*5-1-5 Kashiwanoha, Kashiwa, Chiba 277-8581, Japan*

<sup>9</sup>*Materials Science and Technology Division, Oak Ridge National Laboratory, Oak Ridge, Tennessee 37831, USA*

<sup>10</sup>*Lehrstuhl für Theoretische Physik I, Staudtstrasse 7,*

*Universität Erlangen-Nürnberg, D-91058 Germany*

<sup>11</sup>*Theoretische Festkörperphysik, JARA-FIT and JARA-HPC,*

*RWTH Aachen University, 52056 Aachen, Germany*

(Dated: November 10, 2020)

We present a comprehensive study of the effect of hydrostatic pressure on the magnetic structure and spin dynamics in the spin-1/2 coupled ladder compound  $C_9H_{18}N_2CuBr_4$ . The applied pressure is demonstrated as a parameter to effectively tune the exchange interactions in the spin Hamiltonian without inducing a structural transition. The single-crystal heat capacity and neutron diffraction measurements reveal that the Néel ordered state breaks down at and above a critical pressure  $P_c \sim 1.0$  GPa through a continuous quantum phase transition. The thorough analysis of the critical exponents indicates that such transition with a large anomalous exponent  $\eta$  into a quantum-disordered state cannot be described by the classic Landau's paradigm. Using inelastic neutron scattering and quantum Monte Carlo methods, the high-pressure regime is proposed as a  $Z_2$  quantum spin liquid phase in terms of characteristic fully gapped vison-like and fractionalized excitations in distinct scattering channels.

PACS numbers: 75.10.Jm 75.40.Gb 75.50.Ee

Landau's symmetry-breaking theory [1, 2] has been the cornerstone of understanding phases of matter in condensed matter physics. Despite its remarkable success, various phenomena, including the fractional quantum Hall effect [3, 4] and topologically ordered quantum matter [5, 6] have shown the limitations of this paradigm. Furthermore, continuous zero-temperature quantum phase transitions (QPTs), which exhibit emergent gauge fields and fractionalized (deconfined) degrees of freedom, also extend beyond this conventional framework. In recent years, several model systems, proposed to exhibit deconfined quantum criticality, have been exhaustively studied by analytical [7, 8] and numerical [9–12] methods. However, to the best of our knowledge, thus far there has still been no experimental realization of such unconventional QPT with fractionalization.

The  $S=1/2$  magnetic insulator  $C_9H_{18}N_2CuBr_4$  (DLCB for short) has been synthesized recently [13]. Based on the crystal structure in Fig. 1(a), it is composed of coupled two-leg spin ladders with the chain direction extending along the  $b$ -axis. The inter-ladder coupling in DLCB is sufficiently strong to drive the system to an an-

tiferromagnetically ordered phase below 2.0 K [14]. The staggered moments point alternately along an easy axis ( $\equiv \hat{z}$ ), the  $\mathbf{c}^*$ -axis in the reciprocal space with an ordered moment size of  $0.39(5) \mu_B$ , just 40% of the saturated moment size due to strong quantum fluctuations.

The magnetic excitations of DLCB at ambient pressure can be described quantitatively [15] by the Hamiltonian of a two-dimensional model for the magnetic interactions:

$$H = \sum_{\gamma, \langle i, j \rangle} J_\gamma [S_i^z S_j^z + \lambda (S_i^x S_j^x + S_i^y S_j^y)], \quad (1)$$

where the subscript  $\gamma$  reads either 'rung', 'leg', or 'int'—for  $J_\gamma$  being the rung, leg, or interladder exchange constant—and  $i$  and  $j$  are the nearest-neighbor lattice sites. The parameter  $\lambda$  specifies an interaction anisotropy [16], with  $\lambda=0$  and  $1$  being the limiting cases of Ising and Heisenberg interactions, respectively. Owing to an Ising-type anisotropy, the polarized neutron study [17] confirms that the gapped triplet ( $S=1$  and  $S_z=0, \pm 1$ ) excitation energy splits into a gapped doublet ( $S=1$  and  $S_z=\pm 1$ ) as the transverse mode (TM) and a gapped "singlet" ( $S=1$  and  $S_z=0$ ) as the longitudinal or amplitude mode (LM) [18]

reflecting spin fluctuations perpendicular and parallel to the easy axis, respectively. Importantly, analysis of the spin Hamiltonian suggests that DLCB is close to the quantum critical point (QCP) at ambient pressure and zero field [14, 15, 17, 19] thus its magnetic properties could be extraordinarily responsive to an external stimulus such as hydrostatic pressure.

In this Letter, we present the compelling AC heat capacity and neutron scattering results in DLCB with hydrostatic pressure applied up to 1.7 GPa, which directly detect the magnetic order and dynamic structure factor (DSF) thus allowing us to address the nature of the static and dynamic spin-spin correlations under pressure. Figure 1(b) summarizes the phase diagram of DLCB as determined in this study as a function of temperature and pressure as well as the pressure dependence of anisotropic energy gaps. In the following, we will demonstrate the collapse of the AFM ordering at  $P_c \sim 1.0$  GPa through a continuous phase transition with a large anomalous exponent  $\eta$ , which is strong evidence for fractionalized degrees of freedom. With the aid of quantum Monte Carlo (QMC) calculations, we propose the disordered high-pressure phase as a  $Z_2$  topological spin-liquid phase characterized by the spin-gapped vison-like mode and fractionalized excitation [20].

Figure 1(c) shows the AC heat capacity of a deuterated single crystal of DLCB as a function of temperature [21]. At ambient pressure, a sharp anomaly indicates a phase transition to the AFM state at  $T_N = 2.0$  K. This peak becomes broader and smaller at 0.48 and 0.8 GPa indicative of suppression of the AFM order with increasing pressure and at or above 1.0 GPa it becomes indiscernible at least down to the temperature of 0.15 K. To explore this collapse of the Néel order in more detail, we measured the order parameter of DLCB using the single-crystal neutron diffraction method. Figure 2(a-b) shows the pressure-dependence of neutron diffraction  $\theta/2\theta$  scans at the AFM wavevector  $\mathbf{q} = (0.5, 0.5, -0.5)$ . The scattering intensity of the magnetic Bragg peak becomes diminished as hydrostatic pressure increases. At and above the hydrostatic pressure of 1.05 GPa, there is no experimental evidence of magnetic order down to 0.25 K. Moreover, no evidence is found of any incommensurate magnetic Bragg peak or diffuse scattering over a wide range of reciprocal space at  $T = 0.25$  K and  $P = 1.3$  GPa in Fig. 2(c). The refinement of additional single-crystal neutron diffraction data at and above 1.05 GPa does not reveal any structural distortion as the possible cause for the absence of magnetic order and the triclinic space group  $P\bar{1}$  is preserved at each pressure as listed in Tab. S1 of the Supplementary Material [22]. The temperature-dependent order parameter has been measured at various pressures as well. Figure 2(d) outlines the determined pressure dependence of the ordered moment size  $m$  that is continuously reduced to  $0.08(5) \mu_B$  at 0.95 GPa, indicating a continuous QPT [23, 24]. The best fit to  $m \propto (P_c - P)^\beta$

yields  $P_c = 1.03(3)$  GPa and the order-parameter exponent  $\beta = 0.65(5)$  that is appreciably larger than  $\beta \simeq 0.33$  for the three-dimensional (3D) Ising universality class as expected for the coupled XXZ ladders [25]. A large  $\beta$  is a strong signature of deconfinement at the transition, *i.e.*, the order parameter fractionalizes into partons, and hence the critical exponents differ significantly from the conventional values within the Landau paradigm. It is noteworthy that the determined AFM ordering temperature  $T_N$  increases slightly upon initially increasing pressure and then decreases gradually with pressure until the abrupt change towards zero at  $P_c$ . This behavior is rather distinct from the conventional phase diagram, where  $T_N$  has a smooth power-law decrease towards zero at the critical point. We consider this as an indication that the underlying physics is also distinct from a conventional order-to-quantum disorder transition scenario. As discussed in the Supplementary Material, such apparent sudden drop of  $T_N$  near  $P_c$  can be quantified by a logarithmic behavior as  $T_N \sim 1/\ln(P_c - P)^{-1}$  [22].

In order to gain more insight into the nature of this pressure-induced disordered phase, inelastic neutron scattering has been used to probe the evolution of the dynamic spin-spin correlation function of DLCB as a function of pressure. Figures 3(a) and (b) show the background-subtracted energy scans at the same AFM wavevector for various pressures. The spectral line-shapes for  $P < P_c$  (or  $P > P_c$ ) are spin-gapped and were modelled by superposition of two (or single) double-Lorentzian damped harmonic-oscillator (DHO) models convolved with the instrumental resolution function. At ambient pressure, the best fit yields the gap energies of TM and LM as  $\Delta_{TM} = 0.32(3)$  meV and  $\Delta_{LM} = 0.58(4)$  meV, respectively. Their values are consistent with the previous report [17]. We find that the peak profiles of both TM and LM for  $P \leq 0.82$  GPa are limited by the instrumental resolution. Notably, TM becomes broad at 0.95 GPa with an intrinsic full width at half maximum (FWHM) =  $0.15(4)$  meV. Figure 1(b) summarizes the pressure dependence of the extracted excitation energies  $\Delta_{TM}$  and  $\Delta_{LM}$  across the phase transition. The slightly growing gap energy of  $\Delta_{TM}$  can delay the thermal depletion of the magnetic order to higher  $T_N$ .  $\Delta_{LM}$  becomes softened with a decrease of the ordered moment and the best fit to  $\Delta_{LM} \propto (P_c - P)^\nu$  gives the correlation-length exponent  $\nu = 0.32(4)$  that is much smaller than  $\nu \simeq 0.63$  for the 3D Ising universality class as expected for the coupled XXZ ladders [25]. Notably, recent QMC work finds a similarly small value of  $\nu \simeq 0.45$  at the deconfined QCP in the  $S=1/2$  square-lattice  $J$ - $Q$  model [26, 27]. At 1.06 GPa, slightly above  $P_c$ , LM has a very small gap which cannot be distinguished by the limited instrumental resolution while  $\Delta_{TM}$  moves further to  $0.44(3)$  meV. Based on the spin Hamiltonian at ambient pressure in Eq. (1), the ground state in the quantum disordered phase is expected to be a trivial dimer-

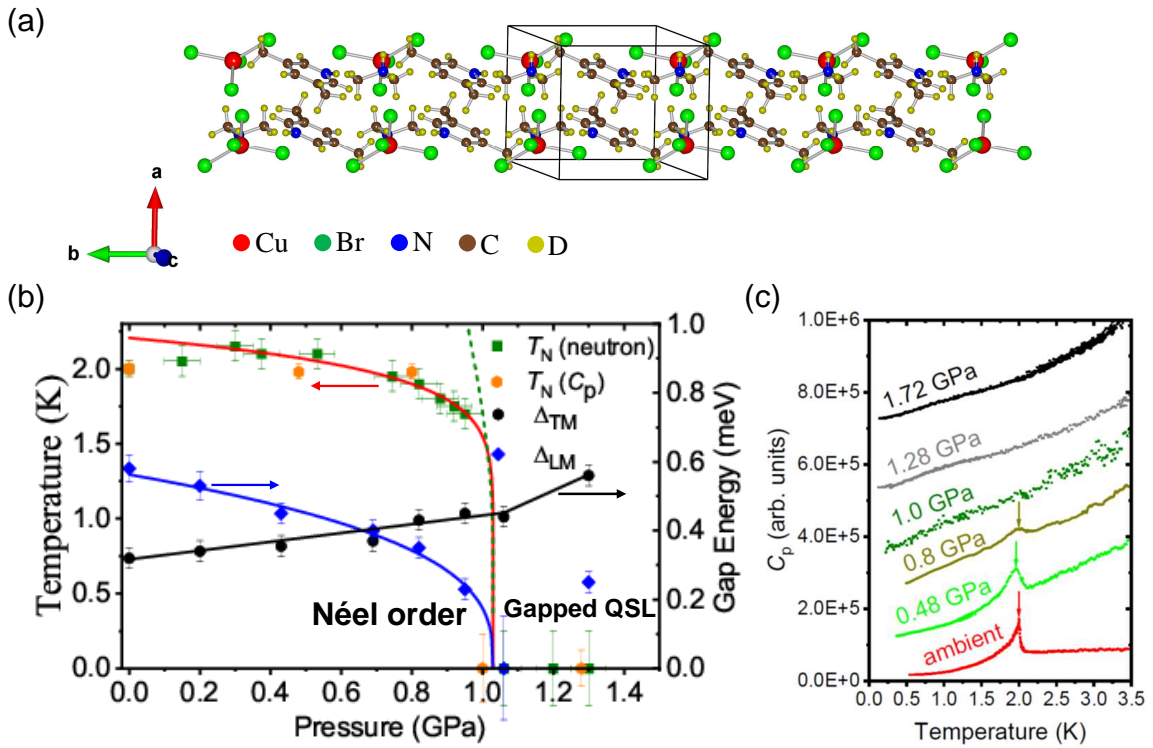


FIG. 1: (a) Crystal structure of deuterated  $C_9H_{18}N_2CuBr_4$  projected along the crystallographic  $c$ -axis to show the stacking of discrete DMA<sup>+</sup> ( $C_2D_8N$ ) and 35DMP<sup>+</sup> ( $C_7D_{10}N$ ) cations. Outlined is a nuclear unit cell. (b) Phase diagram of DLCB as a function of pressure and temperature, including the pressure dependence of anisotropic energy gaps. Circle and diamond points are the energy gaps of the TM and LM, respectively. The red and black solid lines are guides to the eye. The blue line was obtained from a fit of  $\Delta_{LM}(P) \propto (P_c - P)^\nu$  with  $P_c$  fixed at 1.03 GPa and the fitted exponent  $\nu=0.32(4)$ . The olive short-dashed line is obtained from  $T_N(P) \propto 1/\ln(P_c - P)^{-1}$ . (c) The AC heat capacity  $C_p$  of DLCB as a function of temperature at ambient pressure, 0.48, 0.8, 1.0, 1.28 and 1.72 GPa. For clarity, the data are shifted upwards. The transition temperature is indicated by an arrow.

ized quantum paramagnet, where spins are paired into singlet bonds arranged in a regular pattern. Such a phase has sharp excitations. Surprisingly, the spectral line shape of the TM signal becomes significantly broader than the instrumental resolution and the best fit to the same double-Lorentzian DHO model gives an intrinsic linewidth FWHM=0.42(5) meV. Such spectral broadening persists at least up to 1.3 GPa beyond the QCP, where FWHM becomes 0.34(5) meV.

To allow a quantitative comparison to the theoretical characterization of spin dynamics, we examine the DSF using large scale QMC calculations of the same spin Hamiltonian. The Hamiltonian parameters at ambient conditions were obtained to best match the experimentally observed magnetic dispersions as  $J_{leg}=0.62$  meV,  $J_{rung}=0.66$  meV,  $J_{int}=0.20$  meV and  $\lambda=0.87$  [15]. We establish that the applied pressure is effectively tuning the exchange coupling ratio  $\alpha$  between the inter-ladder and intra-ladder couplings and assume no impact on the interaction anisotropy  $\lambda$  and the ratio between  $J_{rung}$  and  $J_{leg}$  (see the Supplementary Material [22] for further details). At the critical point or 1.3 GPa,  $\alpha$  is reduced to

0.14 or 0.05 from 0.32 at ambient pressure and the parameter set ( $J_{leg}=0.91$  meV,  $J_{rung}=0.97$  meV and  $J_{int}=0.13$  meV) or ( $J_{leg}=1.03$  meV,  $J_{rung}=1.1$  meV and  $J_{int}=0.05$  meV) [28] gives the best agreement with the experimental value of  $\Delta_{TM}$ . The calculated spectral lineshape profiles as indicated by the orange lines in Fig. 3(a) are visibly limited by the instrumental resolution. Moreover, Fig. 4 shows the comparison over the entire Brillouin zone between the experimental excitation spectra at 1.06 and 1.3 GPa and DSF calculated by QMC and convolved with the instrumental resolution function. Clearly, the experimental data cannot be reproduced by QMC calculations for the Hamiltonian in Eq. (1).

So what is the probable origin of the continuum-like broad excitation of DLCB? We have carried out single-crystal neutron diffraction experiments under pressure by measuring more than 300 nuclear Bragg peaks and the fitting outcome as listed in Tabs. S2-S5 of the Supplementary Material [22] does not reveal any evidence of chemical disorder under pressure except a small H/D isotope effect on site occupancy. The latter has no influence on the magnetism of non-hydrogen-bonded systems such

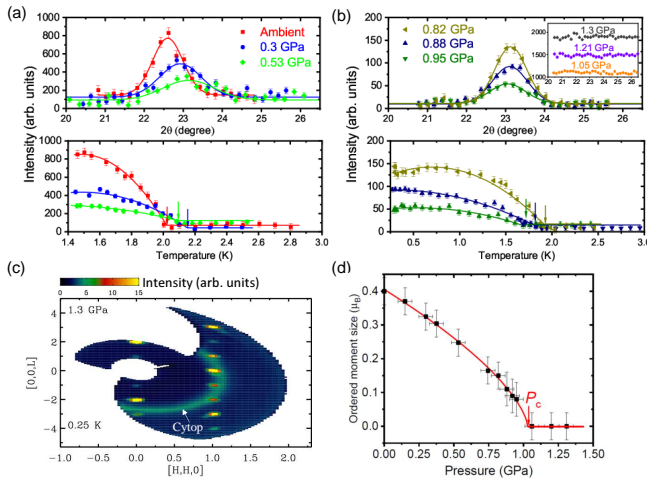


FIG. 2: Single-crystal neutron diffraction study under pressure. The representative  $\theta/2\theta$  scans and the temperature dependence of the neutron scattering intensity measured at CTAX around the antiferromagnetic wavevector  $\mathbf{q}=(0.5,0.5,-0.5)$  for (a) ambient pressure, 0.3 and 0.53 GPa and for (b) 0.82, 0.88 and 0.95 GPa, respectively. For  $\theta/2\theta$  scans, the solid lines are fits to the Gaussian profile. For clarity, the data above 1 GPa presented in the inset are shifted vertically by successive increments of 400. For temperature dependence of the order parameter, the transition temperature at each pressure is indicated by the arrow and the solid lines are guides to the eye. (c) Single-crystal neutron diffraction pattern measured at CNCS at  $T=0.25$  K and  $P=1.3$  GPa. The ring feature is caused by the cytol glue. (d) The determined ordering moment size as a function of applied pressure. The red line below  $P_c$  is a fit of the ordered moment  $m(P) \propto (P_c - P)^\beta$  with the fitted exponent  $\beta=0.65(5)$  and  $P_c=1.03(3)$  GPa. Error bars represent one standard deviation. Experimental data below and above 0.8 GPa were collected at  $T=1.45$  K and 0.25 K, respectively.

as DLCB. Consequently, it can be ruled out that the observed broadening is due to disorder. The other possible broadening effect attributed to spontaneous quasiparticle decays [29, 30] is also discussed in the Supplementary Material [22] and can be excluded mainly due to violation of the kinematic conditions [31]. Moreover, at the critical pressure, the critical exponent  $\eta$  which describes the decay of the correlation function is related to other critical exponents by the scaling law [25]  $\eta = 2\beta/\nu - (d + z - 2)$ , where  $d$  is the number of spatial dimensions and  $z$  is the dynamic critical exponent. Assuming  $d=2$  based on the strong two-dimensional character of the magnetism in DLCB, and  $z=1$  at the pressure-induced quantum phase transition [23], we obtain  $\eta=3.0(5)$  from  $\beta=0.65(5)$  and  $\nu=0.32(4)$  as already stated above. This is in marked contrast to the value  $\eta \approx 0.036$  in the conventional 3D Ising transition [25]. With fractionalization, the Landau order parameter becomes a composite operator of partons, which leads to a large  $\eta$  [12]. The large  $\eta$  can explain the broad spectral linewidth near the transition in DLCB and further suggests that emergence of the

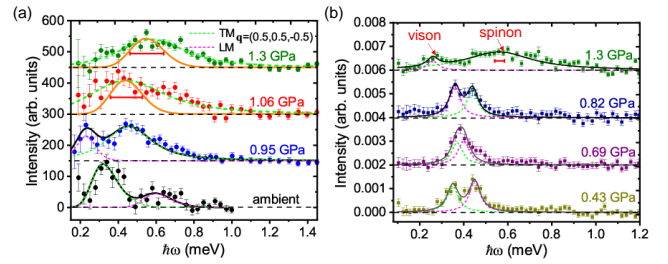


FIG. 3: Single-crystal inelastic neutron scattering study under pressure. The representative background-subtracted transferred energy scans measured at (a) MACS and (b) CNCS at the antiferromagnetic wavevector  $\mathbf{q}=(0.5,0.5,-0.5)$  for several pressures. All data were collected at  $T=1.5$  K except that the data at 1.3 GPa (CNCS) were measured at 0.25 K. For clarity, the data and fits are shifted vertically by successive increments of 150 (MACS) or 0.002 (CNCS). The green and magenta dashed lines are fits to the DHO model convolved with the instrumental resolution for the TM and LM, respectively. The black solid lines are their sum. The green and orange solid lines at 1.06 and 1.3 GPa (MACS) are convolved calculations for the transverse mode by the DHO model and QMC calculations, respectively. The black dashed lines are guides to the eye. The red horizontal bars represent the instrumental resolution. Error bars represent one standard deviation.

gapped phase with fractionalized excitations through this pressure-induced phase transition cannot be described by Landau's paradigm.

Consequently, we propose that the quantum disordered phase with  $P > P_c$  is a gapped quantum spin liquid (QSL) state with fractionalized degrees of freedom. In order to stabilize such a QSL state in DLCB, a mechanism that is not included in the original Hamiltonian is required. Indeed, for unfrustrated interactions, an ordinary quantum phase transition to a trivial quantum paramagnet emerges [23]. The possibility of diagonal frustrating couplings in the ladders can be eliminated due to their unfavorable superexchange paths in DLCB. On general grounds, higher order four-spin interactions such as those around plaquettes are also expected to be negligible for molecular ladder systems. One may also consider further anisotropic exchange terms, the Dzyaloshinskii-Moriya (DM) interactions. In DLCB, DM interactions are forbidden along the rungs of the ladders and between the ladders by the inversion symmetry, but are allowed along the ladder legs. DM anisotropy has been investigated by ESR measurements in other metal-organic ladder compounds including  $(C_5H_{12}N)_2CuBr_4$  (BPCB) [32] and  $(C_7H_{10}N)_2CuBr_4$  (DIMPY) [33, 34], and was found to be about 5% of the dominant exchange interactions. In general, DM interactions prefer non-collinear magnetic structures, and in DLCB the effects of the DM interactions on the collinear ordered state within the Néel phase should thus be very weak. Indeed, the field dependence of the anisotropic energy gaps at ambient pressure [17]

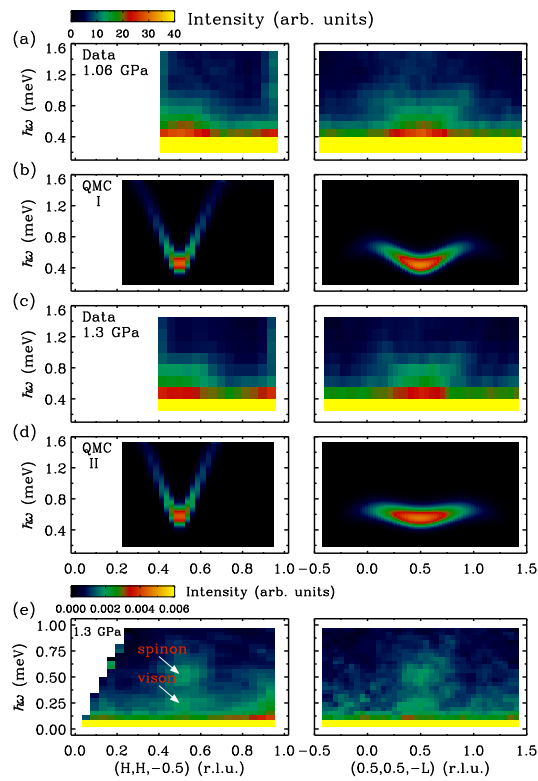


FIG. 4: Comparison between the experimental data and QMC calculations. False-color maps of the excitation spectra as a function of energy and wavevector transfer along two high-symmetry directions  $(H,H,-0.5)$  and  $(0.5,0.5,-L)$  in the reciprocal space, respectively. Experimental data were collected at MACS at  $T=1.5$  K and (a)  $P=1.06$  GPa and (c)  $P=1.3$  GPa. Data for  $H$  less than 0.4 r.l.u. are not shown due to a contamination by the direct neutron beam. (b) and (d) are dynamic structure factors of the TM calculated by QMC using the parameter sets at the critical point and 1.3 GPa, respectively, as described in the text. Simulations were convolved with the instrumental resolution function where the neutron polarization factor and the magnetic form factor for  $\text{Cu}^{2+}$  were included. (e) High-resolution inelastic neutron scattering measurements at CNCS at  $T=0.25$  K and  $P=1.3$  GPa. The excitation spectra at  $T=15$  K are shown in Fig. S4(c) of the Supplementary Material [22]. No smoothing or symmetrization was applied to all experimental data.

agrees well with the Zeeman spectral splitting, which suggests that  $S^z$  is a good quantum number. It is possible, that the effects of the DM interactions become enhanced within the QSL phase. Although we note that a recent study finds that QSL phases can be stable at weak DM interactions [35], further theoretical work is needed to establish the proper lattice Hamiltonian for the entire phase diagram.

One simple example of gapped QSL with fractionalization is the  $Z_2$  spin liquid, which has been shown to exist in quantum dimer model on the triangular lattice [36] and also XXZ spin model on the Kagomé lattice [37]. Such a  $Z_2$  QSL state exhibits non-trivial topological order,

which is characterized by, e.g., the topological degeneracy of the ground states. It furthermore exhibits two primary types of excitations: spinons that carry a  $Z_2$  gauge charge and visons that carry  $Z_2$  gauge flux [38, 39]. These excitations are bosonic, with a semionic mutual statistics. In the easy-axis limit, the visons transform as  $S^z=0$  (singlet) excitations under the  $U(1)$  symmetry about the easy-axis [37], i.e., they reside within the LM channel for DLCB. High-resolution inelastic neutron scattering was used in order to nail down the possible vison excitations deep in the QSL phase. The excitation spectra at  $P=1.3$  GPa in Fig. 4(e) clearly show two well-separated gapped modes including one broad continuum-like and another almost dispersionless excitation. At the AFM wavevector, cf. Fig. 3(b), we clearly identify two distinct excitations: (i) a broad peak at about 0.56(4) meV with a FWHM of 0.36(4) meV, which we identify as arising from fractionalized excitations as spinons, and (ii) an additional, resolution-limited excitation at 0.25(3) meV, identified as the vison excitation.

In summary, we have performed neutron scattering experiments under pressure on DLCB at low temperature and continuously tuned the ground state of the compound  $\text{C}_9\text{H}_{18}\text{N}_2\text{CuBr}_4$  from the AFM Néel state, through an unconventional QPT with a large anomalous exponent  $\eta$ , to an exotic quantum disordered state. By contrasting with QMC calculations for the conventional spin model for DLCB, the unique ability of neutron scattering to probe spin pair correlation functions allows one to experimentally identify fully gapped vison-like and fractionalized excitations consistent with a possible  $Z_2$  QSL state. Our study offers a much-needed experimental platform to search for QSL physics along with the associated quantum criticality within a single compound.

We gratefully acknowledge the helpful discussions with Collin Broholm, Masashige Matsumoto and Guangyong Xu. We are indebted to Cenke Xu for the unique comments and insights. We also thank Matthew Collins, Michael Cox, Saad Elorfi, Cory Fletcher, Juscelino Leão, Christopher Redmon, Christopher Schmitt, Randall Sexton, Erik Stringfellow and Tyler White for the technical support in neutron scattering experiments. A portion of this research used resources at the High Flux Isotope Reactor and Spallation Neutron Source, a DOE Office of Science User Facility operated by the Oak Ridge National Laboratory (ORNL). Access to MACS was provided by the Center for High Resolution Neutron Scattering, a partnership between NIST and NSF under Agreement No. DMR-1508249. The research is also supported by Go! Student Program of ORNL.

\* hongt@ornl.gov

[1] L. D. Landau, Phys. Z. Sowjetunion **11**, 26 (1937).

- [2] V. L. Ginzburg and L. D. Landau, Zh. Eksp. Teor. Fiz. **20**, 1064 (1950).
- [3] D. C. Tsui, H. L. Stormer and A. C. Gossard, Phys. Rev. Lett. **48**, 1559 (1982).
- [4] R. B. Laughlin, Phys. Rev. Lett. **50**, 1395 (1983).
- [5] Xiao-Gang Wen, Rev. Mod. Phys. **89**, 041004 (2017).
- [6] B. Keimer and J. E. Moore, Nat. Phys. **13**, 1045 (2017).
- [7] T. Senthil, A. Vishwanath, L. Balents, S. Sachdev and M. P. A. Fisher *et al.*, Science **303**, 1490 (2004).
- [8] T. Senthil, L. Balents, S. Sachdev, A. Vishwanath and M. P. A. Fisher *et al.*, Phys. Rev. B **70**, 144407 (2004).
- [9] A. W. Sandvik, Phys. Rev. Lett. **98**, 227202 (2007).
- [10] R. G. Melko and R. K. Kaul, Phys. Rev. Lett. **100**, 017203 (2008).
- [11] S. V. Isakov, Y. B. Kim and A. Paramakanti, Phys. Rev. Lett. **97**, 207204 (2006).
- [12] S. V. Isakov, R. G. Melko and M. B. Hastings, Science **335**, 193-195 (2012).
- [13] F. Awwadi *et al.*, Inorg. Chem. **47**, 9327 (2008).
- [14] T. Hong, K. P. Schmidt, K. Coester, F. F. Awwadi, M. M. Turnbull, Y. Qiu *et al.*, Phys. Rev. B **89**, 174432 (2014).
- [15] T. Ying, K. P. Schmidt and S. Wessel, Phys. Rev. Lett. **122**, 127201 (2019).
- [16] In order to minimize the number of fitting parameters to be determined from the experimental dispersion data, we assume that  $\lambda$  is the same for all  $J$ 's. Note that this assumption is made to prevent overparameterization and would not affect the main conclusion of this work.
- [17] T. Hong *et al.*, Nat. Phys. **13**, 638 (2017).
- [18] B. Normand and T. M. Rice, Phys. Rev. B **56**, 8760 (1997).
- [19] T. Hong *et al.*, Nat. Commun. **8**, 15148 (2017).
- [20] C. Broholm, R. J. Cava, S. A. Kivelson, D. G. Nocera, M. R. Norman and T. Senthil, Science **367**, eaay0668 (2020).
- [21] A broad maximum at  $T \simeq 1$  K in the AC heat capacity is observed above  $P_c$ . It is attributed to a Schottky anomaly, which is not indicative of a phase transition but indicative of a gapped ground state with short-range spin correlations.
- [22] See Supplemental Material for details on experimental methods, data analysis, quantum Monte Carlo calculations, the unusual phase boundary near the transition, spontaneous quasiparticle decays and crystal structure and magnetic interactions under pressure.
- [23] S. Sachdev, Quantum Phase Transition (Cambridge Univ. Press, Cambridge, 1999).
- [24] M. Vojta, Rep. Prog. Phys. **66**, 2069 (2003).
- [25] A. Pelissetto and E. Vicari, Phys. Rep. **368**, 549 (2002).
- [26] H. Shao, W. Guo and A. W. Sandvik, Science **213**, 352 (2016).
- [27] A. W. Sandvik and B. Zhao, Chin. Phys. Lett. **37**, 057502 (2020).
- [28] Note that quantum Monte Carlo calculation at 1.3 GPa from a trivial quantum paramagnetic ground state underestimates the actual value of  $J_{\text{int}}$ .
- [29] M. B. Stone *et al.*, Nature **440**, 187 (2006).
- [30] M. E. Zhitomirsky and A. L. Chernyshev, Rev. Mod. Phys. **85**, 219 (2013).
- [31] Y. Su, A. Masaki-Kato, W. Zhu, J.-X. Zhu, Y. Kamiya and S.-Z. Lin, Phys. Rev. B **102**, 125102 (2020).
- [32] E. Cizmar *et al.*, Phys. Rev. B **82**, 054431 (2010).
- [33] V. N. Glazkov, M. Fayzullin, Yu. Krasnikova, G. Skoblin, D. Schmidiger, S. Mühlbauer and A. Zheludev, Phys. Rev. B **92**, 184403 (2015).
- [34] M. Ozerov, M. Maksymenko, J. Wosnitza, A. Honecker, C. P. Landee, M. M. Turnbull, S. C. Furuya, T. Giamarchi and S. A. Zvyagin, Phys. Rev. B **92**, 241113(R) (2015).
- [35] O. Cepas, C. M. Fong, P. W. Leung and C. Lhuillier, Phys. Rev. B **78**, 140405(R) (2008).
- [36] R. Moessner and S. L. Sondhi, Phys. Rev. Lett. **86**, 1881 (2001).
- [37] L. Balents, M. P. A. Fisher and S. M. Girvin, Phys. Rev. B **65**, 224412 (2002).
- [38] T. Senthil and M. P. A. Fisher, Phys. Rev. B **62**, 7850 (2000).
- [39] T. Senthil and M. P. A. Fisher, Phys. Rev. B **63**, 134521 (2001).

---

\* hongt@ornl.gov